Experimental and Theoretical Studies of the Unimolecular Decomposition of Nitrosobenzene: High-Pressure Rate Constants and the C−N Bond Strength

J. Park, I. V. Dyakov, A. M. Mebel,† and M. C. Lin*

Department of Chemistry, Emory University, Atlanta, Georgia 30322

Received: April 9, 1997; In Final Form: June 17, 1997[⊗]

The unimolecular decomposition of nitrosobenzene has been studied at 553−648 K with and without added NO under atmospheric pressure. Kinetic modeling of the measured C_6H_5NO decay rates by including the rapid reverse reaction and minor secondary processes yielded the high-pressure first-order rate constant for the decomposition $C_6H_5NO \rightarrow C_6H_5 + NO$ (1), $k_1^\infty = (1.42 \pm 0.13) \times 10^{17} \exp[-(55\,060 \pm 1080)/RT]$ s^{-1}, where the activation energy is given in units of cal/mol. With the thermodynamics third-law method, employing the values of k_1^∞ and those of the reverse rate constant measured in our earlier study by the cavity ring-down technique between 298 and 500 K, we obtained the C−N bond dissociation energy, $D_0^\circ(C_6H_5-NO) = 54.2$ kcal/mol at 0 K, with an estimated error of ±0.5 kcal/mol. This new, larger bond dissociation energy is fully consistent with the quantum mechanically predicted value of 53.8−55.4 kcal/mol using a modified Gaussian-2 method. Our high-pressure rate constant was shown to be consistent with those reported recently by Horn et al. (ref 13) for both forward and reverse reactions after proper correction for the pressure falloff effect.

I. Introduction

Nitrosobenzene (C_6H_5NO) is a convenient thermal[1−3] and photolytical[4−10] source of phenyl radical. The rate constant for the unimolecular decomposition of nitrosobenzene, $C_6H_5NO \rightarrow C_6H_5 + NO$ (1), was first measured by Choo et al. employing the very-low-pressure pyrolysis (VLPP) method.[11] Their extrapolated high-pressure rate constant by means of the Rice−Ramsperger−Kassel−Marcus (RRKM) theory, $k_1^\infty = 2.5 \times 10^{15} \exp(-24\,660/T)$ s^{-1}, has provided the widely accepted C−N bond dissociation energy $D_{298}^\circ(C_6H_5-NO) = 51 \pm 1$ kcal/mol.[12]

Recently, the unimolecular decomposition of C_6H_5NO was studied by Horn et al.[13] in shock waves in the 800−1000 K temperature range at pressures between 0.9 and 4.4 atm. Their first-order rate constant obtained near 2 atm can be represented by $k_1 = 10^{15.29\pm0.53} e^{-(24720\pm1110)/T}$ s^{-1}, which appears to be in accord with the extrapolated result of Choo and co-workers.[11] Horn et al.[13] have also measured the rate constant for the association of C_6H_5 with NO near 10 Torr in the 420−820 K range using a fast-flow reactor under pseudo-first-order conditions. Their result is in close agreement with that of Yu and Lin obtained by the cavity ring-down (CRD) method.[6]

In order to extend the range of temperature beyond that employed in our phenyl kinetic studies with the CRD technique, 300−523 K,[4−10] we utilized C_6H_5NO as the thermal source of C_6H_5 in the temperature range 553−648 K with and without added NO. For providing a more accurate prediction of C_6H_5 concentration, we have carried out a series of measurements for the rate constant of the C_6H_5NO decomposition reaction by Fourier transform infrared (FTIR) spectrometry. The study was performed under atmospheric conditions, and its result reveals that the activation energy for the decomposition reaction is higher by as much as 6 kcal/mol than those reported earlier.[11,13] In order to confirm this surprising finding, we performed a high-level *ab initio* molecular orbital (MO) calculation, employing the Gaussian-2 method (G2M) recently developed by Mebel and co-workers.[14] The experimental and theoretical results are presented below.

II. Experimental and Computational Procedures

A. Experiment. The rate constant for the unimolecular decomposition of C_6H_5NO was measured at temperatures between 553 and 648 K at atmospheric pressure in a static reactor using the pyrolysis-FTIR (Fourier transform infrared) spectrometric method.[15−17] Pyrolysis was carried out in a 270 cm^3 quartz reactor, housed in a double-walled cylindrical oven. The reactor was heated by adjusting the current through the heater, and the current was controlled by a temperature controller (OMEGA CN 9000). The temperature was measured with a type K thermocouple, located in the center of reactor bulb, with an accuracy and reproducibility of 1 K.

The concentrations of the reactants/products of unpyrolyzed and pyrolyzed samples were taken and analyzed by an FTIR spectrometer (Mattson Instruments, Polaris) with a resolution of 4 cm^{-1}. The concentrations of C_6H_5NO and NO ranged from 0.07 to 0.10% and 0.00 to 0.45%, respectively, with Ar dilution to atmospheric pressure. The concentrations of C_6H_5NO and NO were calibrated with standard mixtures at pressures near those of expanded, pyrolyzed samples. Calibration curves were plotted in terms of concentration versus absorbance at 1113.0 cm^{-1} for C_6H_5NO and 1905.8 cm^{-1} for NO.

C_6H_5NO (Aldrich) was purified by recrystallization using ethanol, followed by vacuum distillation at 273 K to remove the ethanol solvent. NO (Matheson Gas Products) was purified by vacuum distillation through a silica gel trap at 195 K. Before use, the trap was preheated and diffusion-pumped overnight at 420 K to remove any condensed water. Ar (99.9995%, Specialty Gases) was used without further purification.

B. Computation. In order to confirm the measured high-pressure activation energy for the C_6H_5NO dissociation reaction, we have performed *ab initio* molecular orbital calculations for the $C_6H_5NO = C_6H_5 + NO$ system using a modified G2M.[14] The geometries of C_6H_5NO, C_6H_5, and NO have been optimized using the hybrid density functional B3LYP method[18,19] with the 6-31G(d) basis set.[20] Vibrational frequencies, calculated at the

† Present address: Institute of Atomic and Molecular Sciences, Academia Sinica, P.O. Box 23-166, Taipei 10764, Taiwan.

* Key correspondent. Email: chemmcl@emory.edu.

⊗ Abstract published in *Advance ACS Abstracts,* August 1, 1997.

S1089-5639(97)01225-5 CCC: $14.00

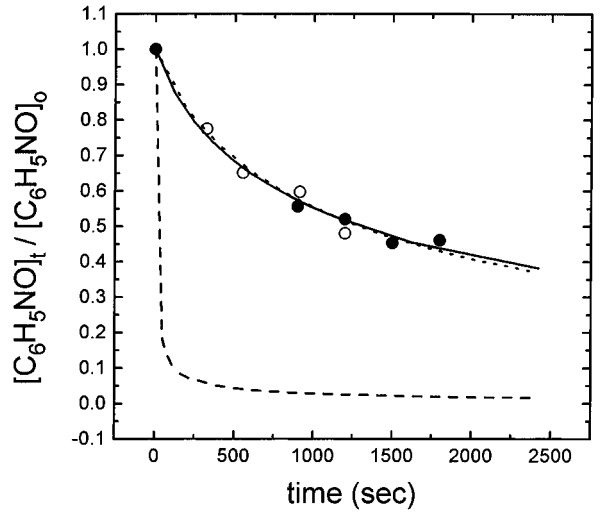

Figure 1. Time-resolved concentration decay profiles of nitrosobenzene: (○) $T = 592$ K without added NO; (●) $T = 650$ K with NO added; (solid line) modeled result at 592 K with $k_1 = 6.06 \times 10^{-4}$ s^{-1}; (dashed line) modeled result at 650 K without added NO using $k_1 = 5.60 \times 10^{-2}$ s^{-1}; (dotted line) modeled result at 650 K with NO added using $k_1 = 5.60 \times 10^{-2}$ s^{-1}.

B3LYP/6-31G(d) level, were used for zero-point-energy (ZPE) corrections, thermal corrections, and Gibbs free energy calculations.

The energies were refined at various levels of theory, such as MP2/6-31G(d,p), MP2/6-311G(d,p), MP2/6-311+G(3df,2p),[20] and coupled-cluster[21] RCCSD(T)/6-31G(d,p) as well as RCCSD(T)/6-311G(d,p). The most accurate energies were obtained by using the G2M(rcc,MP2*) and G2M(RCC,MP2) schemes,[14,22] where

$$E[\text{G2M(RCC,MP2)}] = E[\text{RCCSD(T)/6-311G(d,p)}] + E[\text{MP2/6-311+G(3df,2p)}] - E[\text{MP2/6-311G(d,p)}] + \Delta E(\text{HLC,RCC}) + \text{ZPE}$$

$$\Delta E(\text{HLC,RCC}) = -5.25n_\beta - 0.19n_\alpha \quad \text{in mhartree}$$

$$E[\text{G2M(rcc,MP2*)}] = E[\text{RCCSD(T)/6-31G(d,p)}] + E[\text{MP2/6-311+G(3df,2p)}] - E[\text{MP2/6-31G(d,p)}] + \Delta E(\text{HLC,rcc}) + \text{ZPE}$$

$$\Delta E(\text{HLC,rcc}) = -4.93n_\beta - 0.19n_\alpha \quad \text{in mhartree}$$

Here, n_α and n_β are the numbers of α and β valence electrons, respectively. The G2M approach is expected to provide the bond dissociation energies with an accuracy of 1−2 kcal/mol. GAUSSIAN 94[23] and MOLPRO-96[24] programs were employed for the computations.

III. Results

A. Kinetic Data. The rate constant for the unimolecular decomposition of C_6H_5NO was measured by monitoring the decay of nitrosobenzene concentration as a function of time. At higher temperatures, we added NO into the gas mixture to decrease the decomposition rate of nitrosobenzene. In the NO-added experiments, the [NO]/[C_6H_5NO] ratio varied randomly from 4 to 10 with one [NO] at each temperature. The temperature range was limited by the measurability of the decay rate with and without NO, varying from ∼10 min to ∼10 h (overnight). Typical time-resolved concentration decay profiles of nitrosobenzene are shown in Figure 1.

TABLE 1: Summary of the Experimental Conditions[a] and Rate Constants for the C_6H_5NO Decompostion Reaction at the Temperatures Studied[b]

temp (K)	$[C_6H_5NO]_0$	$[NO]_0$	k_1 (s^{-1})
553	1.64×10^{-8}	0	$(2.91 \pm 0.28) \times 10^{-5}$
563	1.61×10^{-8}	0	$(5.72 \pm 0.58) \times 10^{-5}$
583	1.56×10^{-8}	0	$(2.72 \pm 0.36) \times 10^{-4}$
592	1.18×10^{-8}	0	$(6.06 \pm 0.74) \times 10^{-4}$
598	1.17×10^{-8}	0	$(1.25 \pm 0.66) \times 10^{-3}$
599	1.17×10^{-8}	0	$(1.08 \pm 0.40) \times 10^{-3}$
603	1.53×10^{-8}	0	$(1.75 \pm 0.11) \times 10^{-3}$
608	1.15×10^{-8}	0	$(2.21 \pm 0.09) \times 10^{-3}$
573	1.30×10^{-8}	5.23×10^{-8}	$(1.29 \pm 0.19) \times 10^{-4}$
588	1.51×10^{-8}	6.08×10^{-8}	$(4.35 \pm 0.58) \times 10^{-4}$
605	1.45×10^{-8}	7.81×10^{-8}	$(2.28 \pm 0.36) \times 10^{-3}$
620	1.45×10^{-8}	7.81×10^{-8}	$(6.52 \pm 0.36) \times 10^{-3}$
623	1.42×10^{-8}	5.74×10^{-8}	$(4.69 \pm 0.24) \times 10^{-3}$
623	1.45×10^{-8}	9.88×10^{-8}	$(6.65 \pm 0.24) \times 10^{-3}$
635	1.44×10^{-8}	12.9×10^{-8}	$(1.83 \pm 0.36) \times 10^{-2}$
638	1.24×10^{-8}	8.40×10^{-8}	$(1.97 \pm 0.24) \times 10^{-2}$
645	1.71×10^{-8}	12.9×10^{-8}	$(3.81 \pm 0.36) \times 10^{-2}$
648	1.22×10^{-8}	8.27×10^{-8}	$(2.76 \pm 0.36) \times 10^{-2}$
650	1.69×10^{-8}	17.9×10^{-8}	$(5.60 \pm 0.36) \times 10^{-2}$

[a] The concentration units are in mol/cm^3. [b] All experiments were performed at 1 atm total pressure with Ar as diluent. The error represents 1σ.

TABLE 2: Reactions and Rate Constants[a] for the Modeling of the Nitrosobenzene Decomposition

	reactions[b]	A	E_a	ref
1.	$C_6H_5NO \rightarrow C_6H_5 + NO$	1.42E+17[d]	55 060	this work
−1.	$C_6H_5 + NO \rightarrow C_6H_5NO$	2.69E+12	−860	6
2.	$C_6H_5 + C_6H_5 = C_{12}H_{10}$	1.39E+13	111	31
3.	$C_6H_5 + C_6H_5NO \rightarrow C_{12}H_{10}NO$	4.90E+12	−68	31
−3.	$C_{12}H_{10}NO \rightarrow C_6H_5NO + C_6H_5$	5.00E+14	45 000	*c*
4.	$C_6H_5 + C_6H_5NO \rightarrow C_{12}H_{10} + NO$	5.00E+12	4500	*c*
5.	$C_{12}H_{10}NO + C_6H_5 \rightarrow C_{12}H_{10}N + C_6H_5O$	1.00E+13	0	*c*
6.	$C_{12}H_{10}N + NO \rightarrow C_{12}H_{10}NNO$	1.00E+13	0	*c*

[a] Rate constants are defined by $k = A \exp(-E_a/RT)$ and in units of cm^3, mol, and s; E_a is in units of cal/mol. [b] The equal sign represents that the modeling was carried out for both forward and reverse directions. The arrow represents the forward direction only. [c] Assumed. [d] Read as 1.42×10^{17}.

In order to isolate the unimolecular decomposition rate of nitrosobenzene, we carried out kinetic chemical modeling for each experimental run to account for the competing secondary reactions. The decomposition rate of nitrosobenzene was obtained by fitting the calculated concentrations to our experimentally measured values. The experimental conditions and kinetically modeled data are summarized in Table 1. The reaction mechanism used for kinetic modeling is presented in Table 2. The Arrhenius plot of the modeled unimolecular decomposition rate constants is presented in Figure 2 and compared with previously reported data.[11,13] A weighted least-squares analysis of our data covering the 553−648 K temperature range gave rise to the expression $k_1^\infty = (1.42 \pm 0.13) \times 10^{17} \exp[-(55\,060 \pm 1080)/RT]$ s^{-1}, where $R = 1.987$ cal/(mol K).

B. Theoretical C−N Bond Energy. The calculated energies of C_6H_5NO, C_6H_5, and NO are shown in Table 3, and the molecular parameters for these species are presented in Table 4. The geometry optimization of C_6H_5NO was carried out without symmetry constraints and was converged to a planar structure. As shown in Figure 3, the structure of C_6H_5NO is stabilized by the O···H hydrogen bond between the oxygen of the NO group and a neighboring H. We discussed the optimized geometry of the phenyl radical in an earlier paper.[25] At the B3LYP level with ZPE corrections the C−N bond dissociation

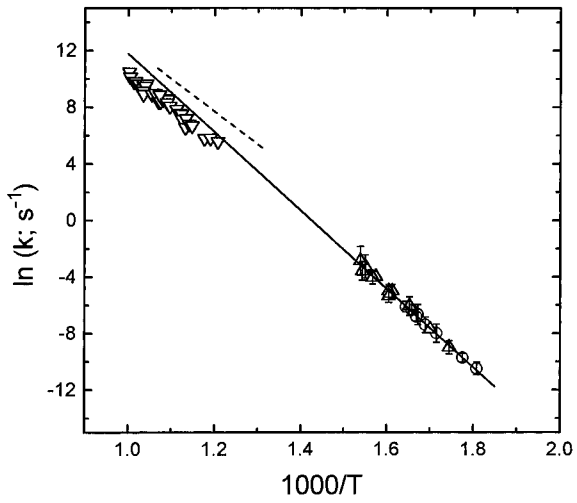

Figure 2. Arrhenius plot of nitrosobenzene unimolecular decomposition reaction: (▽) ref 13; (△) this work with NO added; (○) this work without NO added; (dotted line) ref 11; (solid line) this work according to eq II.

energy was calculated to be 53.2 kcal/mol. The RCCSD(T) approximation gives values in the 49−51 kcal/mol range. The MP2 energies are much higher and are not reliable because of the enormous spin contamination of the UHF wave function for C_6H_5.[25] The G2M(rcc,MP2*) and G2M(RCC,MP2) methods gave close values of 53.8 and 55.4 kcal/mol, respectively. We consider the latter result to be the most accurate one in the present study. After inclusion of the thermal correction for room temperature, we obtained the value of 56.5 kcal/mol for the C−N bond dissociation energy at 298 K.

In order to confirm the result, we also performed the calculation of the enthalpy change for the following isodesmic reaction:

$$C_6H_5NO + H_2 \rightarrow C_6H_6 + HNO$$

At the G2M(RCC,MP2) level, the reaction was calculated to be thermoneutral, $\Delta H_0^\circ = 0.0$ kcal/mol. After adding the thermal corrections, we found $\Delta H_{298}^\circ = -0.8$ kcal/mol. With the experimental heats of formation at 298 K for C_6H_6 and HNO, 19.8 and 25.5 kcal/mol,[26,27] respectively, we calculated $\Delta H_{f,298}^\circ$ for C_6H_5NO as 46.1 kcal/mol. Finally, on the basis of the experimental $\Delta H_{f,298}^\circ$ for NO (21.6 kcal/mol)[28] and C_6H_5 (81.2 kcal/mol),[29] the C−N bond dissociation energy at 298 K is calculated to be 56.7 kcal/mol. Thus, the dissociation energies calculated by the two different approaches are in close agreement. These values are also in good accord with the predicted result of Melius, 57.6 kcal/mol at 298 K, with the BAC-MP4 method.[30]

Using the G2M(RCC,MP2) energy and the molecular parameters of C_6H_5NO, C_6H_5, and NO shown in Table 4, we calculated the equilibrium constant for the $C_6H_5 + NO = C_6H_5NO$ reaction. In the temperature range 300−1000 K, it can be fitted by the following Arrhenius expression:

$$K_{eq} = 2.93 \times 10^{-5} \exp(56\,093/RT)\ \text{cm}^3/\text{mol} \qquad \text{(I)}$$

IV. Discussion

In the temperature range studied, 553−648 K, the decay of C_6H_5NO was found to be dominated by unimolecular decomposition and negatively affected by its reverse reaction:

$$C_6H_5NO \rightleftharpoons C_6H_5 + NO \qquad (1),(-1)$$

with minor contribution from the reaction of C_6H_5 with C_6H_5NO producing biphenyl nitroxide,

$$C_6H_5 + C_6H_5NO \rightarrow (C_6H_5)_2NO \qquad (2)$$

whose rate constant has been determined in this laboratory.[31] In principle, the nitroxide thus formed can react with an additional phenyl radical to produce C_6H_5O and $(C_6H_5)_2N$. Both are thermally stable.

The addition of NO to this highly diluted C_6H_5NO system (%$C_6H_5NO \leq 0.05$) enhances reaction −1 and minimizes the contribution from the secondary and tertiary reactions alluded to above. Figure 1 illustrates the pronounced effect of NO inhibition on the rate of C_6H_5NO decomposition. At 650 K, the half-life of C_6H_5NO is ∼10 s; the addition of 1.8×10^{-7} mol/cm^3 of NO lengthens its half-life to 500 s. Kinetic modeling of the decay of C_6H_5NO, with the inclusion of the secondary and tertiary reactions as summarized in Table 2, enables us to quantitatively obtain the unimolecular decomposition rate constant under the atmospheric pressure of Ar (which corresponds to the high-pressure limit as indicated by Figure 5):

$$k_1^\infty = (1.42 \pm 0.13) \times 10^{17} \exp[-(55\,060 \pm 1080)/RT]\ \text{s}^{-1} \qquad \text{(II)}$$

This result, extrapolated to the 800−1000 K region, lies between those of Choo et al.[11] and Horn and co-workers.[13] The deviation between our values and Horn's results stems from the effect of pressure falloff on Horn's shock tube data (*vide infra*).

The activation energy for the decomposition process, 55.1 kcal/mol, is very close to the C−N bond energy of C_6H_5NO presented in the preceding section, 56.5 kcal/mol at 298 K. The measured activation energy is slightly lower than the bond dissociation energy and is consistent with the negative activation energy, −0.86 kcal/mol, determined for the recombination of C_6H_5 and NO by the cavity ring-down technique.[6] The rate constant for the recombination reaction measured at 20−120 Torr Ar pressure in the 298−500 K range was found to be[6]

$$k_{-1}^\infty = 10^{12.43\pm0.06} \exp[+(860 \pm 220)/RT]\ \text{cm}^3/(\text{mol s}) \qquad \text{(III)}$$

The combination of this reverse rate constant with the equilibrium constant obtained by the *ab initio* calculation presented in the preceding section yields the expression

$$k_1^\infty = k_{-1}^\infty/K_{eq} = 9.2 \times 10^{16} \exp[-55\,230/RT]\ \text{s}^{-1} \qquad \text{(IV)}$$

This result is in excellent agreement with the measured value given by eq II, as also illustrated in Figure 4.

Shown in the figure are the extrapolated high-pressure rate constants of Choo et al.[11] obtained by the VLPP method at 763−953 K and that of Horn et al.[13] measured in shock waves at 800−1000 K. The latter set of data obtained at 0.9-4.4 atm was extrapolated to the high-pressure limit with our high-pressure Arrhenius parameters by the RRKM theory employing the specific rate constant approximated by[32]

$$k_E = A^\infty \rho(E - E^\infty)/h\rho(E) \qquad \text{(V)}$$

where $\rho(E)$ represents the density of the state of C_6H_5NO at energy E and $\rho(E-E^\infty)$, that of C_6H_5NO with energy above the decomposition threshold, which is approximated by $E^\infty = 55.1$ kcal/mol (in lieu of the bond dissociation energy of 0 K, 55.4 kcal/mol). The extrapolation was made with the equation $k_1^\infty = k_1^P/\alpha$, where α is the theoretically predicted falloff ratio, $(k_1^P/k_1^\infty)_T$, at pressure P and temperature T, using the RRKM theory. Under the conditions employed by Horn et al.[13] ($T =$

TABLE 3: Total Energies of C_6H_5NO, C_6H_5, and NO (hartrees) and the C−N Bond Dissociation Energy in C_6H_5NO (kcal/mol), Calculated at Various Levels of Theory

level of theory	C_6H_5NO	C_6H_5	NO	ΔE(C−N)
B3LYP/6-31G(d)	−361.539 80	−231.561 28	−129.888 16	53.2
MP2/6-31G(d,p)	−360.462 15	−230.775 01	−129.553 59	80.3
MP2/6-311G(d,p)	−360.604 92	−230.858 86	−129.617 82	77.0
MP2/6-311+G(3df,2p)	−360.826 48	−231.000 53	−129.692 83	80.0
RCCSD(T)/6-31G(d,p)	−360.549 68	−230.888 71	−129.573 93	51.1
RCCSD(T)/6-311G(d,p)	−360.693 81	−230.969 76	−129.640 12	49.1
G2M(rcc,MP2*)	−360.918 78	−231.098 61	−129.734 43	53.8
G2M(RCC,MP2)	−360.926 54	−231.100 29	−129.737 98	55.4

TABLE 4: Molecular Parameters of C_6H_5NO, C_6H_5, and NO, Calculated at the B3LYP/6-31G(d) Level

species	*i*	I_i (10^{-40} g cm^2)	ν_j (cm^{-1})
C_6H_5NO	*A*	161.2	118,251,258,423,449,477,625,682,695,782,
	B	515.5	836,872,963,995,1015,1019,1045,1105,
	C	676.7	1138,1195,1207,1347,1380,1499,1518,1599, 1653,1665,3191,3204,3211,3221,3230
C_6H_5	*A*	134.8	401,428,601,619,672,722,815,890,958,986,
	B	151.0	988,1023,1058,1081,1182,1183,1313,1342,
	C	285.7	1473,1485,1592,1646,3173,3179,3192,3194,3205
NO	*A*	16.5	1984
	B	16.5	
	C	0.0	

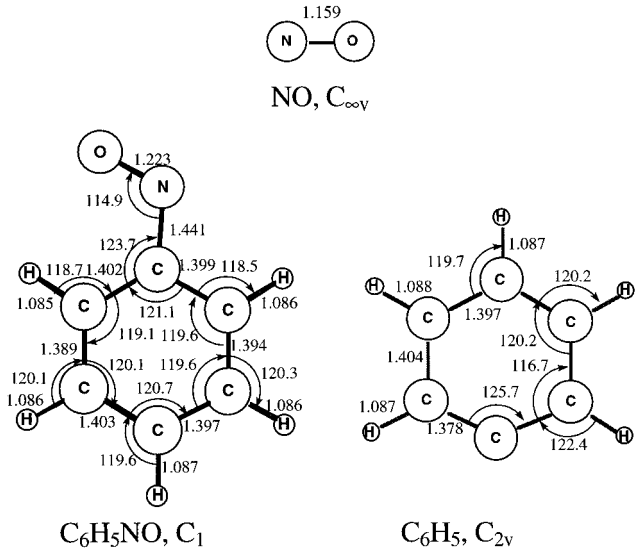

Figure 3. Molecular structures of C_6H_5NO, C_6H_5, and NO calculated with the B3LYP/6-31G(d) method.

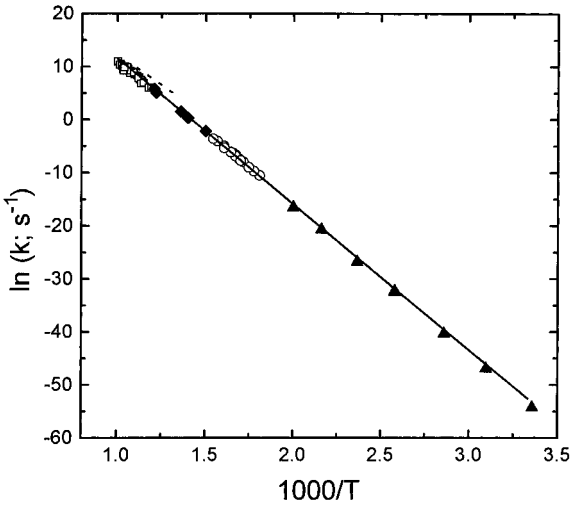

Figure 4. Comparison of the nitrosobenzene decomposition rate after high-pressure-limit correction by the RRKM theory: (▲) k_{-1}^{∞} (ref 6)/K_{eq}; (◆) k_{-1}^{∞} (ref 13)/K_{eq}; (□) ref 13; (○) this work; (dotted line) ref 11; (solid line) this work according to eq II. The pressure-dependent data of ref 13 have been extrapolated to their high-pressure limits, as described in the text.

800−1000 *K*, $P = 0.9-4.4$ atm Ar), the values of α lie between 0.46 and 0.85 with a strong pressure dependence, as illustrated by the pressure falloff plots in Figure 5. The extrapolated values of Horn et al.[13] agree reasonably with our results extrapolated to their temperature region. The result of Choo et al.,[11] however, is noticeably higher than our and Horn's values.

Also shown in Figure 4 are the calculated rate constants, $k_1^{\infty} = k_{-1}^{\infty}/K_{eq}$, using the measured reverse rate constants k_{-1}^{∞} by Yu and Lin[6] as well as Horn et al.[13] with the equilibrium constant K_{eq} given by eq I. With the exception of the highest temperature point, Yu and Lin's values correspond to the high-pressure limits. For the highest-*T* (500 K) result, the falloff ratio was calculated to be $\alpha = 0.95$, which was used in the extrapolation as described above. The results of Horn et al.,[13] measured at 10 Torr total pressure, are well into the falloff region, with $\alpha = 0.99-0.23$ in the 420−820 K range. The data presented in Figure 4 have been approximately corrected for the pressure effect.

In order to obtain reliable experimental values of the enthalpy change for reaction 1, we have employed the thermodynamics third-law method[33] using the equilibrium constant, calculated with the combination of individual rate constant k_{-1}^{∞} reported by Yu and Lin[6] and k_1^{∞} given by eq II for the temperature range of 300−500 K. The results of this evaluation for ΔH_0° with the calculated Gibbs energy function, $-(G_T^{\circ} - H_0^{\circ})/RT$, employing the molecular parameters presented in Table 4, are summarized in Table 5. The averaged value of ΔH_0°, 54.2 kcal/mol with an estimated total error of ±0.5 kcal/mol arising from the scatters of the forward and reverse rate constants, agrees excellently with theoretical values 53.8 and 55.4 kcal/mol based on the two different schemes of G2M calculations. The predicted values are expected to have an uncertainty of 1−2 kcal/mol, as indicated earlier.

V. Conclusion

Our study of the thermal decomposition of C_6H_5NO in the 553−648 K temperature range under atmospheric conditions by FTIR spectrometry gave rise to the high-pressure first-order rate constant for the decomposition process, $C_6H_5NO \rightarrow C_6H_5$

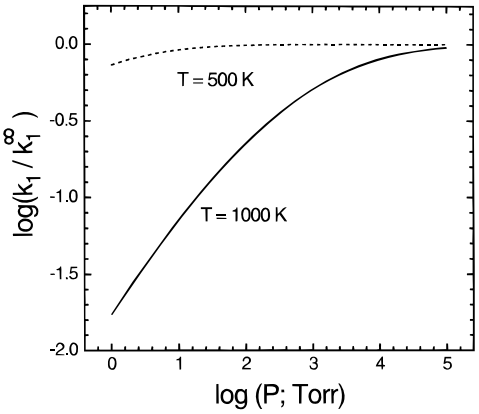

Figure 5. Effect of pressure on the first-order rate coefficient, k_1, at the two temperatures indicated.

TABLE 5: Calculated Values of ΔH_0° by the Third-Law with the Calculated Gibbs Energy Function

temp (K)	k_{-1} (cm^3/mol s)[a]	k_1 (s^{-1})[b]	ΔH_0°(kcal/mol)
298	1.13×10^{13}	5.89×10^{-24}	54.40
323	1.11×10^{13}	7.87×10^{-21}	54.38
350	9.40×10^{12}	5.89×10^{-18}	54.24
388	8.37×10^{12}	1.37×10^{-14}	54.10
388	1.02×10^{13}	1.37×10^{-14}	54.25
388	1.11×10^{13}	1.37×10^{-14}	54.32
423	6.38×10^{12}	5.05×10^{-12}	53.81
463	9.13×10^{12}	1.45×10^{-9}	54.04
500	8.19×10^{12}	1.21×10^{-7}	53.86
average value			54.16 ± 0.22

[a] Data of Yu and Lin, ref 6. [b] Calculated by eq II.

+ NO (1), $k_1^\infty = (1.42 \pm 0.13) \times 10^{17} \exp[-(55\,060 \pm 1080)/RT]$ s^{-1}. The combination of this new result with that reported earlier by Yu and Lin for the reverse process (−1) obtained by the cavity ring-down technique yielded with the third-law method the C−N bond dissociation energy D_0° (C_6H_5−NO) = 54.2 ± 0.5 kcal/mol. This result, after thermal correction to 298 K, is 4 kcal/mol higher than the accepted value, 51 ± 1 kcal/mol.[12] Our higher value is fully consistent with the result of high-level *ab inito* MO calculations, 53.8−55.4 kcal/mol, based on a modified Gaussian-2 method.[14] Furthermore, our high-pressure rate constant k_1^∞ was found to be in good agreement with the results of k_1 and k_{-1}, reported by Horn and co-workers,[13] after appropriate corrections were made for the pressure falloff effect.

Acknowledgment. We acknowledge the support received from the Department of Energy, Office of Basic Energy Sciences, Division of Chemical Sciences, through Contract DE-FGO5-91ER14191. The authors are thankful to the Cherry L. Emerson Center for Scientific Computation for the use of various programs and computing facilities. Helpful discussion with Dr. C. F. Melius is much appreciated.

References and Notes

(1) Lin, C.-Y. Ph.D. Dissertation, The Catholic University of America, Washington, DC, 1987.

(2) Lin, C.-Y.; Sanders, W. A.; Umstead, M. E.; Lin, M. C. Poster paper, *21st Symp. (Int.) Combust.*, Munich, Germany, 1986.

(3) Braun-Unkoff, M.; Frank, P.; Just, Th. *22nd Symp. (Int.) Combust., [Proc.]* **1988**, p 1053.

(4) Yu, T.; Lin, M. C. *J. Am. Chem. Soc.* **1993**, *115*, 4371.

(5) Lin, M. C.; Yu, T. *Int. J. Chem. Kinet.* **1993**, *25*, 875.

(6) Yu, T.; Lin, M. C. *J. Phys. Chem.* **1994**, *98*, 2105.

(7) Yu, T.; Lin, M. C. *Int. J. Chem. Kinet.* **1994**, *26*, 771.

(8) Yu, T.; Lin, M. C.; Melius, C. F. *Int. J. Chem. Kinet.* **1994**, *26*, 1095.

(9) Yu, T.; Lin, M. C. *J. Am. Chem. Soc.* **1994**, *116*, 9571.

(10) Yu, T.; Lin, M. C. *J. Phys. Chem.* **1995**, *99*, 8599.

(11) Choo, K.-L.; Golden, D. M.; Benson, S. W. *Int. J. Chem. Kinet.* **1975**, *7*, 713.

(12) McMillen, D. F.; Golden, D. M. *Annu. Rev. Phys. Chem.* **1982**, *33*, 439.

(13) Horn, C.; Frank, P.; Trauter, R. S.; Schaug, J.; Grotheer, H.-H.; Just, Th. *26th Symp. (Int.) Combust., [Proc.]*, in press

(14) Mebel, A. M.; Morokuma, K.; Lin, M. C. *J. Chem. Phys.* **1995**, *103*, 7414.

(15) He, Y.; Kolby, E.; Shumaker, P.; Lin, M. C. *Int. J. Chem. Kinet.* **1989**, *21*, 1015.

(16) Aldridge, K. H.; Liu, X; Lin, M. C.; Melius, C. F. *Int. J. Chem. Kinet.* **1991**, *23*, 947.

(17) Diau, E. W. G.; Halbgewachs, M. J.; Smith, A. R.; Lin, M. C. *Int. J. Chem. Kinet.* **1995**, *27*, 855.

(18) (a) Becke, A. D. *J. Chem. Phys.* **1993**, *98*, 5648; (b) *Ibid.* **1992**, *96*, 2155; (c) *Ibid.* **1992**, *97*, 9173.

(19) Lee, C.; Yang, W.; Parr, R. G. *Phys. Rev. B* **1988**, *37*, 785.

(20) Hehre, W.; Radom, L.; Schleyer, P. v. R.; Pople, J. A. *Ab Initio Molecular Orbital Theory*; Wiley: New York, 1986.

(21) (a) Purvis, G. D.; Bartlett, R. J. *J. Chem. Phys.* **1982**, *76*, 1910. (b) Hampel, C.; Peterson, K. A.; Werner, H.-J. *Chem. Phys. Lett.* **1992**, *190*, 1. (c) Knowles, P. J.; Hampel, C.; Werner, H.-J. *J. Chem. Phys.* **1994**, *99*, 5219. (d) Deegan, M. J. O.; Knowles, P. J. *Chem. Phys. Lett.* **1994**, *227*, 321.

(22) Liu, R.; Morokuma, K.; Mebel, A. M.; Lin, M. C. *J. Phys. Chem.* **1996**, *100*, 9314.

(23) Frisch, M. J.; Trucks, G. W.; Schlegel, H. B.; Gill, P. M. W.; Johnson, B. G.; Robb, M. A.; Cheeseman, J. R.; Keith, T.; Petersson, G. A.; Montgomery, J. A.; Raghavachari, K.; Al-Laham, M. A.; Zakrzewski, V. G.; Ortiz, J. V.; Foresman, J. B.; Cioslowski, J.; Stefanov, B. B.; Nanayakkara, A.; Challacombe, M.; Peng, C. Y.; Ayala, P. Y.; Chen, W.; Wong, M. W.; Andres, J. L.; Replogle, E. S.; Gomperts, R.; Martin, R. L.; Fox, D. J.; Binkley, J. S.; Defrees, D. J.; Baker, J.; Stewart, J. P.; Head-Gordon, M.; Gonzalez, C.; Pople, J. A. *GAUSSIAN 94*, Revision B.2; Gaussian, Inc.: Pittsburgh, PA, 1995.

(24) MOLPRO is a package of *ab initio* programs written by H.-J. Werner and P. J. Knowles, with contributions from J. Almlöf, R. D. Amos, M. J. O. Deegan, S. T. Elbert, C. Hampel, W. Meyer, K. Peterson, R. Pitzer, A. J. Stone, P. R. Taylor and R. Lindh.

(25) Mebel, A. M.; Lin, M. C.; Yu, T.; Morokuma, K. *J. Phys. Chem.*, in press.

(26) *CRC Handbook of Chemistry and Physics*, 74th ed.; Lide, D. R., Ed.; Chemical Rubber: Boca Raton, FL, 1993.

(27) Dixon, R. N. *J. Chem. Phys.* **1996**, *104*, 6905. The value given at 0 K, 26.29 ± 0.06 kcal/mol, was corrected for the thermal effect. The 298 K value, 25.5 kcal/mol, is very close to 25.4 + 0.6/−0.1 kcal/mol, recommended by W. R. Anderson (CPIA Pub. No. 606, Vol. II, p 205, 1993).

(28) Chase, M. W., Jr.; Davles, C. A.; Downey, J. R., Jr.; Frurip, D. J.; McDonald, R. A.; Syverud, A. N. JANAF Thermochemical Tables. *J. Phys. Chem. Ref. Data* **1985**, *14*, Suppl. 1.

(29) Davico, G. E.; Bierbaum, V. M.; Depuy, C. H.; Ellison, G. B.; Squires, R. R. *J. Am. Chem. Soc.* **1995**, *117*, 2590.

(30) Melius, C. F. BAC-MP4 Heats of Formation and Free Energies, April 25, 2993 (private communication).

(31) Park, J.; Lin, M. C. *J. Phys. Chem.* **1997**, *101A*, 14.

(32) Frost, W. *J. Phys. Chem.* **1972**, *76*, 342

(33) Pitzer, K. S. *Thermodynamics*, 3rd ed.; 1995; McGrawHill: New York, p 114.